

# THE MEGAELECTRON-VOLT ULTRAFAST ELECTRON DIFFRACTION EXPERIMENT AT TSINGHUA UNIVERSITY\*

R. K. Li<sup>†</sup>, C. X. Tang, Y. C. Du, W. H. Huang, H. B. Chen, T. B. Du, Q. Du, J. R. Shi and L. X. Yan  
 Department of Engineering Physics, Tsinghua University, Beijing, China 100084  
 X. J. Wang, NSLS, Brookhaven National Laboratory, Upton, NY 11973, USA

## Abstract

Time-resolved megaelectron-volt ultrafast electron diffraction (MeV UED) will be a powerful tool for structural dynamics studies with a sub-ångström spatial resolution and a  $\sim 100$  femtosecond time-resolving capacity. A MeV UED system mainly consists of an ultrafast laser system and a photocathode RF gun. We evaluate the overall performance of such a system, including the spatial resolution and temporal resolution, based on the laser and electron beam parameters, as well as some hardware performances, e.g. the RF to laser timing jitter. A prototype MeV UED was designed, built and commissioned. We also discuss some hardware and operation issues that are critical to the overall system performance.

## INTRODUCTION

The electron has long been used as a unique probe to peer into the microscopic world, especially since the conventional electron diffraction, crystallography and microscopy were combined with ultrafast laser technologies [1]. State-of-the-art time-resolved ultrafast electron diffraction (UED) employ laser-initialized, direct-current (DC) accelerated 30-60 keV ultrashort electron pulses, and are already possessing picosecond, sub-ångström temporal and spatial resolutions [2, 3, 4].

To improve the temporal resolution to  $\sim 100$  femtosecond level, which is the fundamental time scale of atomic motions, sub-100 fs high quality electron pulses must be generated in the first place. While, due to the strong space-charge effects at keV range, a sub-100 fs electron pulse can only contain no more than a few hundred electrons [5, 6]. It is thus very difficult to achieve  $\sim 100$  fs diffractions with high enough signal-to-noise ratio, in the context of expose time, potential radiation damage of the sample and stability of the apparatus. Moreover, the single-shot  $\sim 100$  fs diffraction is beyond the reach of keV UEDs.

It was then proposed to use MeV electron pulses, for which the space-charge effects are dramatically mitigated, for the UED application [7, 8]. It is possible to encompass  $\sim 1 \times 10^6$  electrons in a single 100 fs MeV pulse. Previous hours expose time with keV UEDs can be reduced to a few seconds or even a single-shot. This greatly facilitates studies on irreversible structural transitions.

\* Supported by the National Natural Science Foundation of China (NSFC) Nos. 10735050, 10875070, and 10805031, and by the National Basic Research Program of China (973 Program) No. 2007CB815102.

<sup>†</sup> lrk@mails.thu.edu.cn

The proposed MeV UED facility consists mainly of a photocathode radio-frequency (RF) gun and an ultrafast laser system, as shown in Fig.1. Electron pulses are initialized by specially tailored ultra-violet (UV) laser pulses, and rapidly accelerated by high gradient RF fields to MeV range. The RF deflecting cavity is used for electron pulse length measurement and other advanced manipulations [9]. Previous simulation [10] and experimental [11, 12] works encouragingly demonstrated the feasibility of MeV UED.

Using numerical simulations, we further optimized the performance of MeV UED, including the spatial and temporal resolutions, by properly choosing the laser and electron beam parameters [13]. A prototype MeV UED system was designed, built and commissioned at the Tsinghua Thomson scattering X-ray sources (TTX) [14]. In this paper, we discuss evaluations of the spatial and temporal resolutions, and some important hardware and operation issues affecting the system performance.

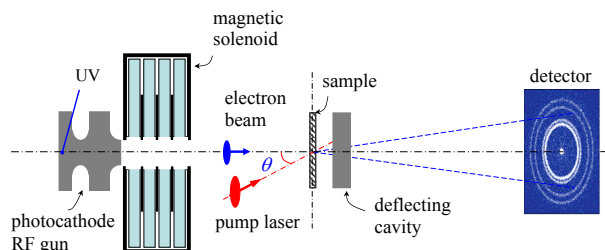


Figure 1: Schematic of a MeV UED system.

## ESTIMATED SYSTEM PERFORMANCES

The simulation strategy, the optimized parameters and diffraction patterns, particularly the physical design of a prototype MeV UED were presented in Ref. [13]. In this section, we discuss our understandings on how to evaluate the performance of a MeV UED system, in terms of the spatial and temporal resolutions.

### Spatial Resolution

The spatial resolution characterizes the precision of the microscopic length that can be interpreted from the measured diffraction pattern. For a polycrystalline sample, the theoretical diffraction pattern consists of a group of concentric rings, each of which is labeled with the Miller indices ( $hkl$ ) and corresponds to a lattice plane of the sample.

The radius of each ring is given by Bragg's law as

$$r = \frac{\lambda}{a_0} L (h^2 + k^2 + l^2)^{1/2}, \quad (1)$$

where  $\lambda$  is the de Broglie wavelength of the electron,  $a_0$  is the structure constant of the sample, and  $L$  is the distance between the sample and the detection plane. The spatial resolution is estimated to be

$$(M \Delta a / a_0)^2 = (\Delta L / L)^2 + (\Delta \lambda / \lambda)^2 + (\Delta r / r)^2, \quad (2)$$

where  $M$  denotes the square-root term in Eq.1. The first two terms on the right-hand-side of Eq.2 can be easily experimentally determined to be better than  $1 \times 10^{-3}$ .

For cases where one ring is clearly resolved from others, its radius can be determined, by averaging and fitting, to a precision of a few micrometers. Thus the term  $\Delta r / r$  is also below  $1 \times 10^{-3}$ . The micro-structure which corresponds to this ring can then be determined as precisely as 0.1 picometer.

However, if two adjacent rings are not resolved, as the cases in previous MeV UED experiments where the adjacent (111) and (200) rings of a polycrystalline aluminum foil broadened to display one single ring-like structure. The broadening might stem from the finite spot-size, divergence and space-charge effects of the electron pulses. The radius of each ring can not be determined better than half of the width of the ring-like structure, and  $\Delta r / r$  is on the order of 10%. The spatial resolution is then merely about 1 Å. It is thus impossible to track the evolution of each ring during an ultrafast structural transition, or even to correctly interpret the static structure.

### Temporal Resolution

The temporal resolution  $\tau$  of MeV UED was analyzed in detail in Ref.[15]. The  $\tau$  is evaluated as [16]

$$\tau = (\sigma_l^2 + \sigma_e^2 + \sigma_{jitter}^2 + \sigma_{vm}^2)^{1/2}, \quad (3)$$

where  $\sigma_l$  is the pump laser pulse duration,  $\sigma_e$  is the probe electron pulse duration,  $\sigma_{jitter}$  is the jitter of the time interval between the pump and probe pulses arriving at the sample, and  $\sigma_{vm}$  stems from the group velocities mismatch of the two pulses in the sample.

Since the laser pulses that pump the sample and those driving the photocathode usually come from a common laser system, they are jitter free and taken as the time reference. The time-of-flight of the electron pulse from the cathode to the sample depends on the phase the RF field, so does the velocity compression of the electron pulse, thus there is a correlation between  $\sigma_{jitter}$  and  $\sigma_e$ . Also, the instability of the RF amplitude makes an contribution. We demonstrated that, with now technically available parameters as the pump laser pulse duration of  $\sigma_l = 50$  fs (rms), the UV laser pulses of  $\sigma_{UV} = 100$  fs (rms), the RF to laser timing jitter  $\sigma_{RL} = 100$  fs (rms), and the RF amplitude instability  $\delta E_{a,rms} = 0.1\%$ , the temporal resolution  $\tau$  is already  $\sim 100$  fs (rms).

### Sources and Injectors

#### T02 - Lepton Sources

## HARDWARE AND OPERATION ISSUES

### Bunch Charge and Dark Current

Space-charge (SC) effects cause expansion of electron pulses in both the transverse and longitudinal directions, which is of negative impacts on the spatial and temporal resolutions. Moreover, SC effects contaminate the information carried by electrons which is gained during the scattering process, e.g. cause increases in the ring radii, which will lead to misinterpretation of the structure of the sample. Thus the bunch charge density should be kept a very low level. According to our simulation optimization result, a 300  $\mu\text{m}$  rms spot-size, 100 fs rms duration electron pulse is typically of a bunch charge of 0.1 pC, or a current of 1 A.

Together with the carefully tailored photo-electron pulses, there is dark current due to the field emission, which depends the RF field amplitude, the material properties and the vacuum condition. The dark current is of a wide energy spectrum. With the optimized operation parameters of the photocathode RF gun and the solenoid, a notable amount of dark current within a certain energy span may hit the sample. The state of the sample may be severely altered due to the radiation damage.

A small fraction of the electrons are transported through the long distance to the detector. Efforts should be made to ensure that the dark current which arrives the detector during the expose time does not notably exceeds the 0.1 pC level. Otherwise, reference patterns should be taken with the sample off the electron beam-line, and then subtracted from those with the sample in.

### Efficiency of the Detection System

As discussed above, to realize a high spatial resolution and a  $\sim 100$  fs temporal resolution, each electron pulse contains roughly  $1 \times 10^6$  electrons. To obtain a single-shot diffraction pattern with high enough signal-to-noise ratio, we require the detection efficiency to approach 100%. Also, the spatial resolution of the detection system should be better than about 50  $\mu\text{m}$ . A commonly used strategy is to first convert the electrons to photons, and then to image the optical signal. There are commercially available electron-multiplying (EM) CCD camera which can catch single photon. The challenges then remain to choose a scintillator with high efficiency, adequate spatial resolution and proper decay time. The microchannel-plate (MCP) which is able to detector the electrons directly with sufficient spatial resolution can be considered as an alternative choice for the detection system, or at least integrated with other elements to form an image-intensifier, just as those used in keV UEDs.

In the prototype MeV UED system, a cerium-doped YAG crystal is placed perpendicular to the electron beam-line. The optical signal is reflected by a 45° metal mirror, and then imaged onto an Andor iXon<sup>EM</sup>+ EMCCD camera. We successfully recorded a high quality diffraction

pattern by accumulating 200 electron pulses [17]. The expose time was set to 10  $\mu$ s, which is the minimum value allowed by the camera. There was still considerable background signal, which may consist of the dark current, the stray light from the UV laser and some viewports, as well as the X-rays generated from the collisions of the electrons with the 45° metal mirror. We planned to replace the YAG crystal with a phosphor screen which is supposed to be of much higher efficiency. The expose time has to be increased to millisecond range accordingly to accommodate the longer decay time of the phosphor. Extra efforts have to be made to reduce the background noise.

### Impact of Field Errors

To correctly interpret the measured diffraction pattern, we need a full understanding of the electron optics between the sample and the detection plane. We designed a free drift space between the sample and the detector in the prototype system. This 411 cm long drift space mainly consist of a 3-meter,  $\Phi$ -63 mm (inner diameter) pipe, an S-band 3-cell deflecting cavity, and a chamber for beam diagnostics, as shown in Fig.2. A pair of steering coils were installed at the entrance of the 3-meter pipe, to correct the potential alignment errors.

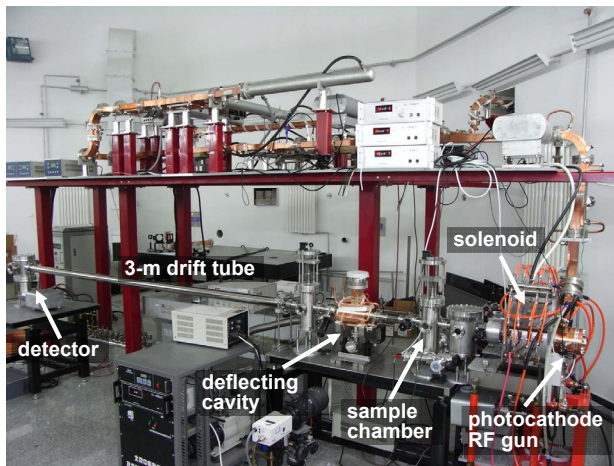


Figure 2: Photo of the prototype MeV UED system.

Contrary to the expected field free space, there exist residual magnetic fields of the beam-line elements, the earth's magnetic field, and the errors of steering coils other than the expected pure dipole mode. Assuming that the earth's magnetic induction strength is vertical and has a value of 0.5 Gauss, and a 2 MeV electron crosses the geometric axis of the 3-meter beam pipe at the entrance and the exit, the electron must travel along a curved trajectory in the horizontal plane, and be roughly 1.2 cm off-axis at the 1.5 m position. At this location, the radius of the (311) diffraction ring of polycrystalline aluminum is already  $\sim$ 1 cm.

We observed in experimental an interesting feature that the recorded diffraction rings were elliptical rather than cir-

cular. We suspected and confirmed with simulation that this was induced by the quadrupole field component of the steering coils. The quadrupole field focuses the electron beam in one transverse direction and defocuses in the other transverse direction. The simulation showed that for 2 MeV electrons, a 0.02 T/m  $\times$  5 cm quadrupole field transforms a circle into an ellipse with a minor-major axes ratio of 0.8. Proper post-processing technique allows correct extraction of the structural information from the transformed elliptical rings [17].

### SUMMARY

In this paper, we discuss the spatial and temporal resolution of MeV UED system. By properly choosing the initial UV laser pulses parameters, the operation parameters of the photocathode RF gun and the solenoid, and improving the hardware performance, e.g. the RF to laser timing jitter and the stability of the RF power, we can reach 0.1 picometer and  $\sim$ 100 fs resolutions. A prototype MeV UED system were built and commissioned. We also present some technical considerations and experiences on how to fulfill a powerful and reliable MeV UED system.

### ACKNOWLEDGMENTS

The authors thank Drs. J. Cao, Y. T. Li and W. X. Liang for many helpful discussions.

### REFERENCES

- [1] G. Mourou and S. Williamson, Appl. Phys. Lett. **41**, 44 (1982).
- [2] D. Shorokhov and A. H. Zewail, Phys. Chem. Chem. Phys. **10**, 2879 (2008).
- [3] J. R. Dwyer *et al.*, Phil. Trans. R. Soc. A **364**, 741 (2006).
- [4] S. Nie *et al.*, Phys. Rev. Lett. **96**, 025901 (2006).
- [5] A. Gahlmann, S. T. Park and A. H. Zewail, Phys. Chem. Chem. Phys. **10**, 2894 (2008).
- [6] X. Wang *et al.*, Rev. Sci. Instrum. **80**, 013902 (2009).
- [7] X. J. Wang, Z. Wu and H. Ihee, in Proceedings of PAC'03, p. 420.
- [8] X. J. Wang *et al.*, J. Korean Phys. Soc. **48**, 390 (2006).
- [9] P. Musumeci *et al.*, Rev. Sci. Instrum. **80**, 013302 (2009).
- [10] F. M. Rudakov *et al.*, AIP Conf. Proc. **845**, 1287 (2005).
- [11] J. B. Hastings *et al.*, Appl. Phys. Lett. **89**, 184109 (2006).
- [12] P. Musumeci, J. T. Moody and C. M. Scoby, Ultramicroscopy **108**, 1450 (2008).
- [13] R. K. Li *et al.*, Chin. Phys. C **33** Suppl. II (2008).
- [14] C. X. Tang *et al.*, in Proceedings of the ICFA Workshop on Compton Sources for X/gamma Rays: Physics and Applications, Alghero, Italy, 7-12 Sept. 2008.
- [15] R. K. Li and C. X. Tang, doi:10.1016/j.nima.2009.03.236 (2009).
- [16] J. C. Williamson and A. H. Zewail, Chem. Phys. Lett. **10** 209 (1993).
- [17] R. K. Li *et al.*, to be submitted.